Manuscript submitted to: Volume 2, Issue 2, 184-199.

AIMS Biophysics DOI: 10.3934/biophy.2015.2.184

Received date 20 March 2015, Accepted date 21 May 2015, Published date 15 June 2015

Review

Structural studies of T4S systems by electron microscopy

Adam Redzej, Gabriel Waksman, and Elena V Orlova*

Institute of Structural and Molecular Biology, University College London and Birkbeck, Malet Street, London WC1E 7HX, UK

*** Correspondence:** Email: e.orlova@mail.cryst.bbk.ac.uk.

Abstract: Type IV secretion (T4S) systems are large dynamic nanomachines that transport DNA and/or proteins through the membranes of bacteria. Analysis of T4S system architecture is an extremely challenging task taking into account their multi protein organisation and lack of overall global symmetry. Nonetheless the last decade demonstrated an amazing progress achieved by X-ray crystallography and cryo-electron microscopy. In this review we present a structural analysis of this dynamic complex based on recent advances in biochemical, biophysical and structural studies.

Keywords: T4S system; electron microscopy; structural analysis; mechanism of action

1. Introduction

All types of bacteria studied so far (Gram-negative, Gram-positive, cell wall-less bacteria) and a number of archaea have revealed the presence of specialised secretion systems that are vital for their survival, pathogenicity and ability to adapt to changes in the environment [1]. These macromolecular machineries are responsible for the transport of DNA and effector molecules across the cell envelope. Secretion systems found in bacteria are currently classified into seven major classes [2–7]. The variety of substrates secreted by type IV secretion (T4S) systems and their nature (single proteins, protein complexes, DNA and nucleoprotein complexes) singles out these secretion systems from the others and make them the most functionally versatile class. Many T4S systems have been shown to

inject (translocate) proteins into the cytosol of eukaryotic cells, where these proteins facilitate bacterial pathogenesis by specifically interfering with host cell function [2–12].

Depending on their function, T4S systems can be divided into three major groups. The first group includes T4S systems that transfer DNA unidirectionally from donor to recipient cell in a contact dependent way. Another group of T4S systems mediates the translocation of proteins, ranging from small protein effectors to large protein complexes. Pathogenic Gram-negative bacteria such as *Helicobacter pylori, Brucella suis* and *Legionella pneumophila* use the T4S system to inject virulence proteins into mammalian host cells [8,9,10] while *Bordetella pertussis* use the T4S systems to secrete pertussis toxin into the extracellular milieu [11]. As a result they cause different types of diseases e.g. respiratory diseases-like "whooping cough", chronic gastric disorders or tumour growth in plants. The last and smallest group consists of T4S systems, which secrete or uptake DNA into or from the extracellular milieu, respectively. *H. pylori* and *Neisseria gonorrhoeae* are examples of bacteria with this type of T4S systems [12,13].

The first type of translocation related to DNA greatly contributes to the spread of antibiotic resistant genes among bacterial species and allows them to adapt to environmental changes. Members of this group are called conjugative type IV secretion systems. The phenomenon of conjugation in bacteria is an enormous public-health problem since this mechanism allows rapid dissemination of antibiotic-resistant genes and other virulence behaviour among pathogens. While the fact that DNA can move from one cell to another was established a long time ago [14,15], the mechanism of secretion is still poorly understood. However, structural information recently obtained allows better understanding of the type IV secretion systems architecture [16]. The revelation of the principles of action of these bacterial nanomachines has broad clinical importance not only due to delivery of bacterial toxins or effector proteins straight into targeted host cells, but for the direct involvement in the rapid horizontal spread of antibiotic resistance genes among the microbial population. In this review we describe the latest progress in structural studies of the T4S system using methods of electron microscopy.

2. Overall Organisation of the Type IV Secretion System

All T4S systems are evolutionarily related and share some structural features such as a specific channel spanning the cell envelope, through which the secreting process occurs in an ATP-dependent manner [17]. Numerous T4S systems are organized similarly to the VirB/D4 *Agrobacterium tumefaciens* system, which is composed of 12 proteins VirB1-VirB11 and VirD4 [18]. This nomenclature is used throughout this review. These proteins assemble into a complex with three distinct substructures: pilus, secretion channel and coupling protein (Figure 1). Other T4S systems which have evolved additional subunits and might be structurally organized in a different way than the VirB/D4 *A. tumefaciens* system e.g. *L. pneumophila* Dot/Icm and *H. pylori* cag system are not discussed in this review.

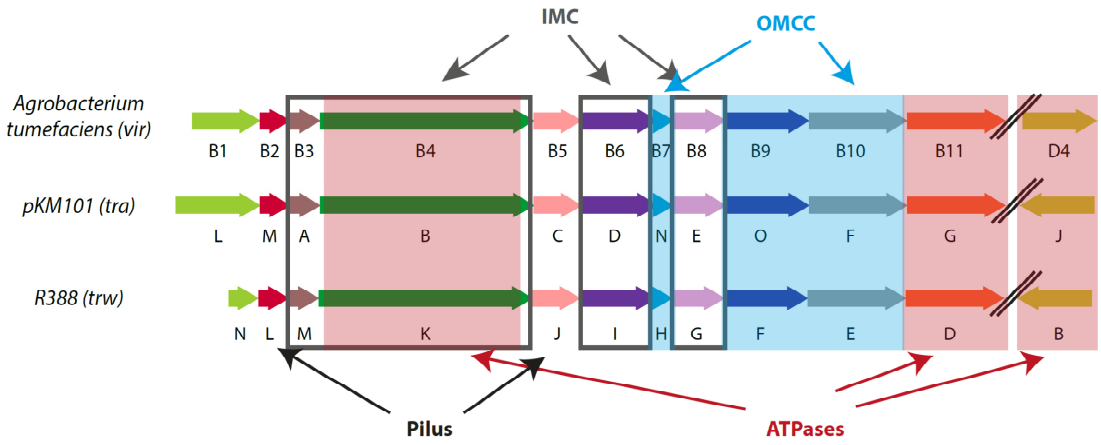

Figure 1. Conserved gene architecture between *A. tumefaciens VirB/D4, E. coli* pKM101 plasmid and *E.coli* R388 plasmid T4S systems.

The pilus is an extracellular appendage, which connects the donor and recipient cell during the DNA transfer—conjugation [1]. Pilus is built up from two proteins, the major subunit VirB2 and the minor subunit VirB5. While multiple copies of VirB2 form a rod like structure, VirB5 can be found at the tip of the pili [19,20]. VirB2 is a small hydrophobic protein, which is proteolytically processed at its termini and polymerizes into a pilus [21]. Alternatively following proteolysis the N-termius and C-terminus of VirB2 is fused resulting in a cyclic peptide [22]. VirB5 is a periplasmic protein with an N terminally located signal peptide sequence. In order for VirB5 to form a complex with VirB2, VirB4 is required [23]. By studying various complexes of VirB4 and VirB5 it has been proposed that VirB4 enable assembly of VirB2 with VirB5 by stabilizing VirB8 and VirB10 complex [23]. Also VirB4 mediates VirB2 assembly into the pilus by extraction from the IM [24]. The structure of VirB5 has been solved by X-ray crystallography [25].

The secretion channel, which in Gram-negative bacteria spans both outer and inner membranes, is composed of an inner-membrane complex (IMC), attached to an outer-membrane core complex (OMCC) via a flexible stalk region (Figure 2). The OMCC is composed of 14 copies of 3 proteins VirB10, VirB9 and VirB7 [26]. It forms a channel, which is inserted in both inner and outer membrane, thereby spanning the whole bacterium envelope. Lipidation of VirB7 is required for anchoring of the OMCC in the outer membrane. The structural details of OMCC are discussed below.

The organisation of the stalk region is yet to be defined. However, it has been suggested that it consists of the N-terminal extensions of VirB10 that stretches out from OMCC towards the inner membrane. Pillus subunits are also likely comprise part of the stalk, or at least pass through the stalk during the pilus polymerization reaction. The IMC contains proteins VirB3, VirB4, VirB6 and VirB8, present in 12, 12, 24 and 12 copies respectively [27] (Figures 1 and 2). VirB3 protein, which is an inner -membrane protein with both N- and C- terminus facing the cytoplasm, is the smallest component of the IMC. For its stability VirB3 requires the presence of VirB4, VirB7, VirB8. VirB3

has been recently shown to form a complex with VirB4 [28]. Interestingly, several genome-sequencing studies have identified a fusion protein between VirB3 and VirB4. VirB6 is a polytopic inner membrane protein with a periplasmic N terminus, five transmembrane segments and a cytoplasmic C terminus [29]. It has been shown in immunofluorescence microscopy experiments that VirB6 localizes to cell poles. Additionally the co-localization of VirB6 with VirB3 and VirB9 has been documented [30]. The proposed function of VirB6 is to regulate T-pilus formation by interactions with VirB5. VirB6 protein also participates in the formation of a complex between VirB7 and VirB9 proteins. VirB8 is a bitopic protein with its N terminus localized in cytoplasm while the C terminus resides in the periplasm [31]. VirB8 interacts with VirB10 and VirB4 and positively regulates the stability of VirB1, VirB3, VirB4, VirB5, VirB6, VirB7 and VirB11 in the *A. tumefaciens* VirB/D4 system [32]. Structures of the periplasmic domain of VirB8 from *Brucella suis* and *A. tumefaciens* have been solved by X-ray crystallography [33,34]. VirB1 is responsible for the lysis of the peptidoglycan cell wall required for the type IV secretion complex insertion [28].

The IMC is powered by three hexameric ATPases on the cytosolic and IM sides: VirB4, VirB11 and VirD4 [35] (Figures 1 and 2). VirB4 is the most conserved T4S system component [36]. Typically it has two domains, the C-terminal domain being more conserved and responsible for ATPase activity while the N-terminal domain is presumably used for the interactions with the IMC of the T4S system. However, VirB4 has only recently been identified within the assembled complex [27]. Even though in some cases transmembrane regions were predicted within the N-terminal part of VirB4, the full-length protein was isolated from both membrane and cytoplasmic fractions. The oligomerization state of the protein remains unclear so far as it has been documented as monomeric, dimeric, trimeric, and hexameric complexes [36,37,38]. However, in a complex with other inner membrane components of the T4S system, VirB4 has been shown to form hexamers [27] (Figure 2). The crystal structure of the C-terminal domain of a homolog of VirB4 from a thermostable organism, *Thermoanaerobacter pseudethanolicus*, has been solved [36].

VirB11 is a soluble hexameric ATPase, which is divided into N- and C-terminal domains by a flexible linker [39]. As the closest structural homologues to VirB11 are AAA^+ ATPases, which are involved in trafficking, it might be that VirB11 behaves like a chaperone, unfolding substrates and being involved in their translocation [40]. It has been suggested that VirB11 is regulating pilus biogenesis by interacting with VirB4 [35].

VirD4 is responsible for the recruitment of the substrate and is therefore often called a coupling protein. It is inserted into the inner membrane via two transmembrane helices [41,42]. VirD4 is known to interact in the cytosol with other ATPases VirB11 and VirB4 and with VirB10 in the IM. The crystal structure of the soluble part of VirD4 from R388 system reveals a hexameric structure [43].

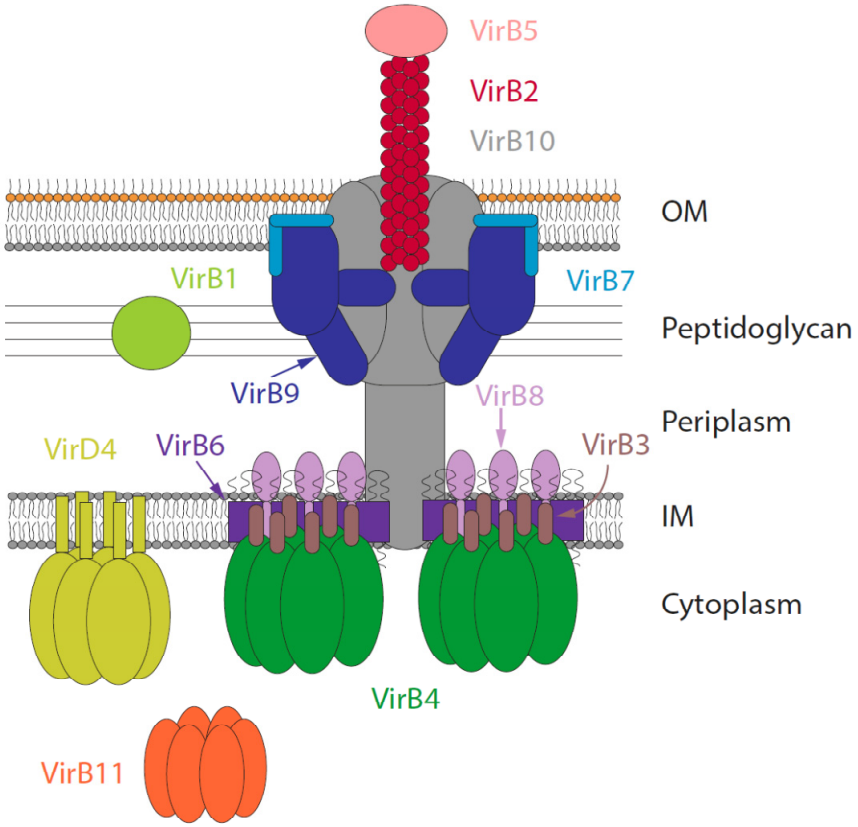

Figure 2. General organisation of the T4S system. On the cytosolic side, three ATPases: VirD4 (in yellow), VirB11 (in orange), VirB4 (in green). Localized in the inner membrane: polytopic VirB6 (in purple), bitopic VirB8 (in light purple) and VirB3 (in brown). OMCC components: VirB7 (in light blue), VirB9 (in blue), and VirB10 (in grey). Pilus subunits: VirB2 (in red) and VirB5 (in salmon). The lytic transglycosylase VirB1 (in light green).

3. Electron Microscopy and Hybrid Methods in Analysis of the T4S System Structural Organisation

Due to their intricacy multi-protein complexes are difficult candidates for structural studies, in particular when they are associated with membranes. In this case electron microscopy is the method of choice. This technique allows visualization of large complexes both within cells and in an isolated form under nearly native conditions [44]. The simplest way of examining the complexes in EM is negative staining (NS). The sample is spread on a support film and covered with a solution of NS (typically a salt of heavy atoms), which is more dense compared to the biological specimen itself [45]. This simple approach allows very quick examination of samples. However owing to the size of the stain grain, flattening effect due to drying at the time of sample preparation, and

sometimes partial staining of the specimen, many structural details in images remain obscured. In order to obtain high-resolution structures of macromolecular assemblies, cryo EM techniques are used [46] where a sample is nearly instantly frozen in aqueous solution at liquid nitrogen temperatures. This allows observing biological complexes close to their native conditions. Here we report analysis of T4S systems using both NS and cryo methods (Figures 3 and 4).

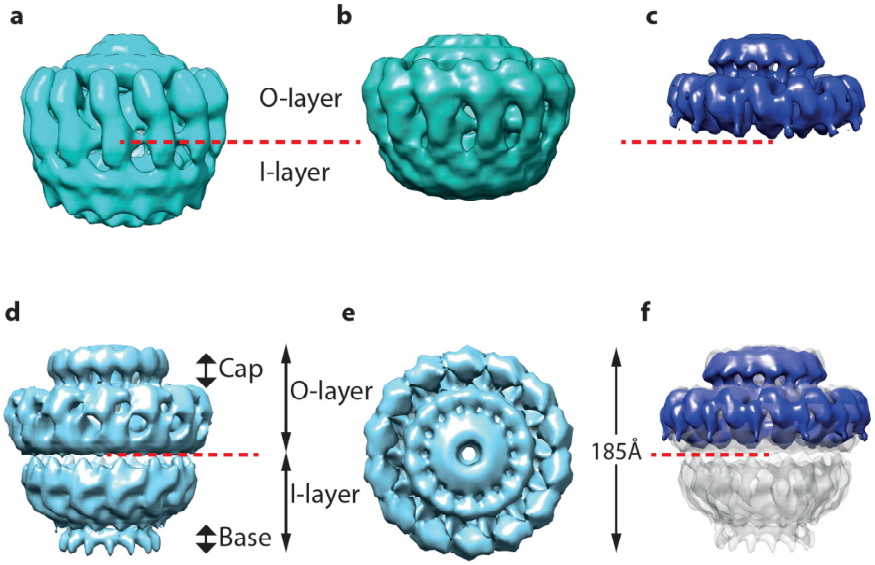

Figure 3. NS-EM structures of the pKM101 OMCC (a) (EMD-5032), the partially trypsin-digested OMCC (b) (EMD-5033) and the fully trypsin-digested OMCC (c) (EMD-5034). (d) A side view and (e) a top view of the cryo-EM structure of pKM101 OMCC obtained at 15 Å resolution (EMD-5031). (f) Overlay of the fully trypsin-digested OMCC structure and the cryo-EM map of the pKM101 full length OMCC.

4. Structure of the OMCC

A first assembly of T4S systems that has been isolated and structurally characterized was the OMCC from pKM101 plasmid [26] (Figure 1). This large complex is composed of 14 copies of each proteins VirB7, VirB9 and VirB10 and has a molecular mass of ~1.1 MDa. The first NS EM reconstruction has revealed a ring like structure with 14-fold symmetry [26] (Figure 3a). Two layers can be clearly distinguished within this structure: the so-called O-layer consisting of a main body topped by a cap and the so-called I-layer below it. In order to identify the localization of the N-terminus of VirB10 within the structure, the full-length OMCC was subjected to mild proteolysis. As a result, a truncated version of the OMCC was obtained with 156 amino acids cleaved from the N-terminus of VirB10 using trypsin (Figure 3b). The only difference between the EM maps of the full

OMCC and the truncated complex is the disappearance of part of the base in the latter one. This indicates that the N-terminal part of VirB10 is localized at the base of the OMCC.

The cryoEM structure of the full-length OMCC has been obtained at ~15 Å resolution and revealed more structural details [26] (Figure 3d–e). The structure clearly demonstrates a two-layer organisation: the upper layer, the 85 Å high O-outer and the 85 Å high I-inner layer, named referring to the position of the layers with respect to the outer and inner membranes. The overall dimensions of the complex are 185 Å both in width and length. Similarly to the negative stain structure of the OMCC, the O-layer includes a cap on top of a main body. The I-layer of the complex ends with a so-called base. Both the I-layer and O-layer have the I-chamber and the O-chamber (Figure 3f). The internal wall of the O-chamber forms a 20 Å wide opening within the cap area, which narrows down to 10 Å on the top of the O-layer. The inner parts of the O- and I-chambers have a diameter of ~60 Å at widest points. The I-chamber narrows to 55 Å at its base [26] (Figure 3f). Further information about the localization of all the proteins within the OMCC has been obtained by digestion of the core complex with trypsin. This led to a formation of a ~500 kDa stable complex, where both VirB9 and VirB10 have been truncated at the N-terminus. The I-layer part of the OMCC was no longer present within the cryoEM reconstruction of the trypsin-digested complex (Figure 3c). Thus it has been concluded that the I-layer is exclusively composed of the N-terminal parts of VirB9 ($VirB9_{NT}$) and VirB10 ($VirB10_{NT}$). The position of the N-terminus of TraF/VirB10 has been localized within the base of the complex by antibody labelling [26].

Later, an improved cryoEM map of the pKM101 full-length OMCC has been obtained at 12.4 Å resolution and revealed new features that were not identified previously [47] (Figure 1, Figure 4a,b). It has been found that the I-layer of the complex has a double-walled structure (Figure 4b). The inner wall diameter varies between 50 and 55 Å and is composed by 14 columns of density separated by 7 Å (Figure 4c, d). The columns are ~8 Å in a diameter and 70 Å in height. The tops of the columns are connected to the O-layer, while their lower parts form the base of the OMCC. More details were revealed in the cryo-EM reconstruction of an elastase-digested OMCC that was obtained at an 8 Å resolution [47] (Figure 4c, d). This complex lacked the first 160 residues of VirB10. Similarly to the trypsin-digested complex, part of the base structure is not present in the elastase-digested OMCC. Moreover, the structures of the I-layer differ between the full-length and elastase-digested OMCC (Figure 4d–e). In the elastase-digested complex, the opening to the cytoplasmic side is wider −65 Å and the inner wall of the I-layer is not present (Figure 4e, d). The composition of the O-layer within the elastase-digested complex has been defined by fitting of the X-ray structure of the ternary complex between VirB7 and the C terminal domains of VirB10 ($VirB10_{CT}$) and VirB9 ($VirB9_{CT}$) (Figure 5a, b) In addition, three helical peptides have been identified based on the sequence of $VirB10_{NT}$ as well as two regions rich in β-strands within the $VirB9_{NT}$ and successfully fitted within the EM map of the full length OMCC. Two of the peptides derived from $VirB10_{NT}$ have been fitted within the inner wall of the I-layer whereas the remaining peptide was found within the base. At the

same time the VirB9$_{NT}$ model has been nicely fitted within the outer wall of the I-layer of the map (Figure 5) [47].

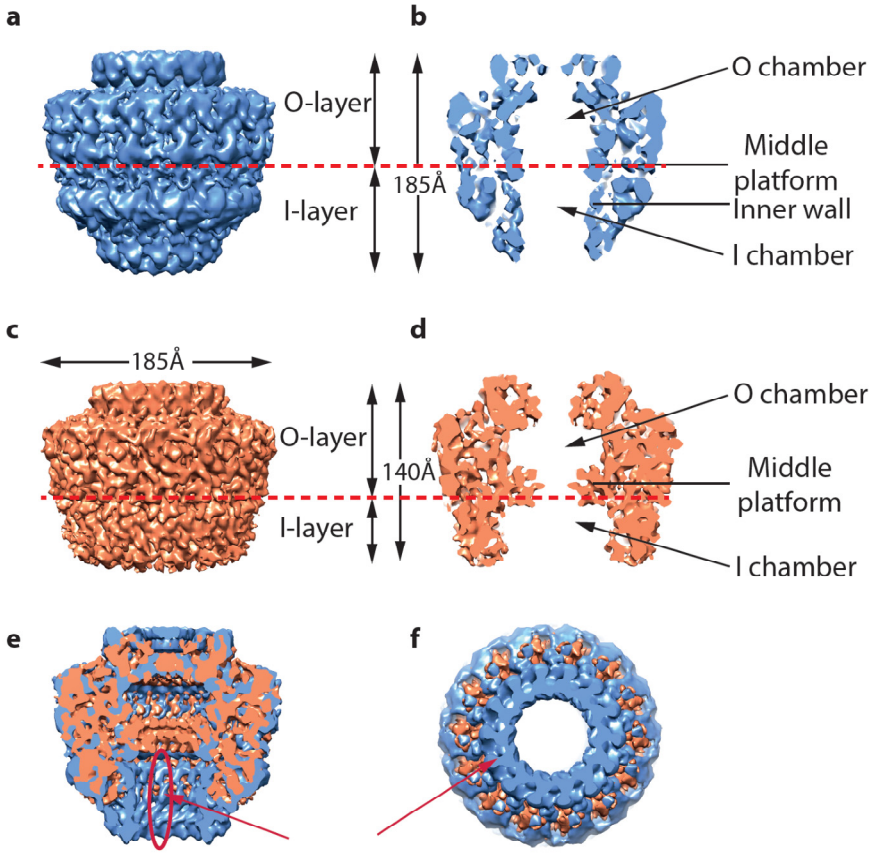

Figure 4. Cryo-EM structures of the pKM101 OMCC (EMD-2232) obtained at 12.4 Å and elastase-digested pKM101 OMCC (EMD-2233). (a,b) Side view and a central section, respectively, of the cryo-EM structure of the OMCC. (c,d)Side view and a central section, respectively, of the cryo-EM structure of the elastase-digested OMCC. (e) Cutaway view of the superposition of the cryo-EM maps of the full-length OMCC (blue) and elastase-digested OMCC (orange) complexes. (f) A cross section of the two superimposed structures in the area of the I-layer. Red oval and arrows indicate positions of columns of the inner wall.

5. First Structural Insight into a Nearly Entire T4S Secretion Assembly

The latest EM reconstruction of the nearly whole T4S system from the R388 plasmid, lacking only the ATPases VirB11 and VirD4 and the major pilus subunit VirB2, shed light into the architecture of the T4S apparatus. The ~3 MDa complex, hereafter called T4SS$_{3\text{-}10}$ is composed of 8 proteins. It has been expressed in *E. coli* and isolated from membranes using affinity purification and

finally visualized by NS-EM [27]. The reconstruction shows three distinct structural parts of the complex: OMCC, IMC and the stalk region that holds them together. The complex is 340 Å in length and 255 Å at its widest point (Figure 6).

The structure of the OMCC within $T4SS_{3\text{-}10}$ is consistent with the structure of the previously described OMCC of the pKM101 plasmid (Figure 1). Importantly the negative stain EM reconstruction of the R388 OMCC on its own is structurally similar to that of the pKM101 (Figures 7a and 7b). 14-fold symmetry of the OMCC has been clearly identified, as well as its separation into two layers (I and O). Interestingly the OMCC within the $T4SS_{3\text{-}10}$ has an inner central stalk that was not observed previously.

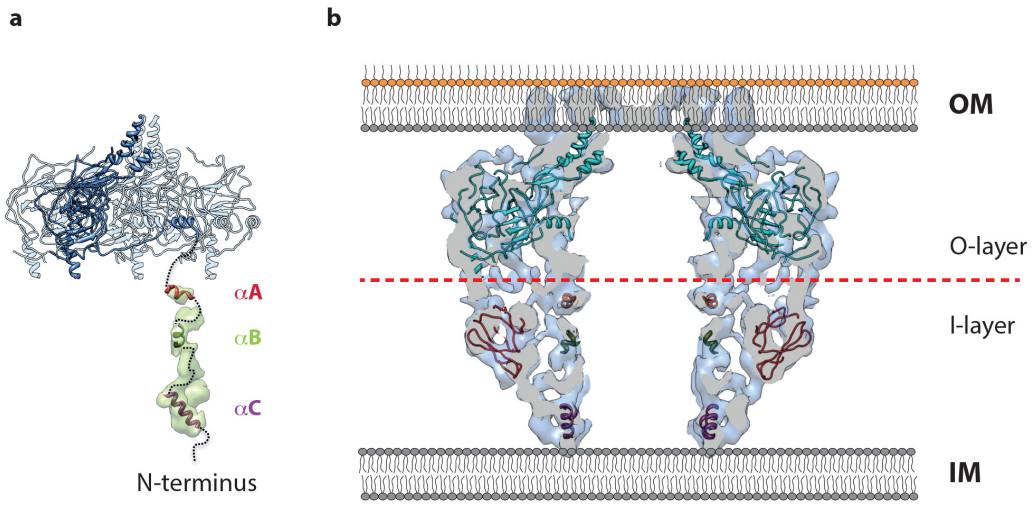

Figure 5. Structural organisation of the OMCC. (a) Four pKM101 $VirB10_{CT}$ subunits (PDB 3JQO) of the 14-mer present in the O-layer atomic structure are shown. One subunit is highlighted in blue. The density of one subunit column is shown in light green. A tentative docking of the three pKM101 $VirB10_{NT}$ α-helical regions is shown within this density. The connections are shown as dashed lines. (b) Central slice of OMCC with fitted O-layer atomic structure (in cyan, PDB 3JQO) and atomic models obtained for $VirB9_{NT}$ from pKM101 plasmid (in dark red) and the α-helices predicted in $VirB10_{NT}$ from pKM101 plasmid (PDB 2YPW).

The IMC is formed of three main parts (Figure 6): the arches, the trans-membrane platform, and two barrel-like structures. Each of the barrels is composed of three tiers called L-tier, M-tier and U-tier. Both L-tier and M-tier display 3 fold symmetry (Figures 6 and 7). The barrels are related by two-fold symmetry. Two T4S system components VirB4 and VirB6 have been localized within the barrel and the IMC platform, respectively, by gold labelling experiments [27]. The length of a monomer of VirB4, corresponds to the length of the two barrels of IMC [27]. Indeed the recently

reported NS-EM reconstruction of the full-length VirB4 from the R388 plasmid shows high level of similarity with the two barrels present within the IMC [37]. Interestingly VirB4 in the absence of other T4S system components appears to be different in size, 165Å long, with a diameter between 132 Å and 124 Å [37], compared to 134 Å in height and ~105 Å in diameter in the $T4SS_{3\text{-}10}$ complex (Figure 6).

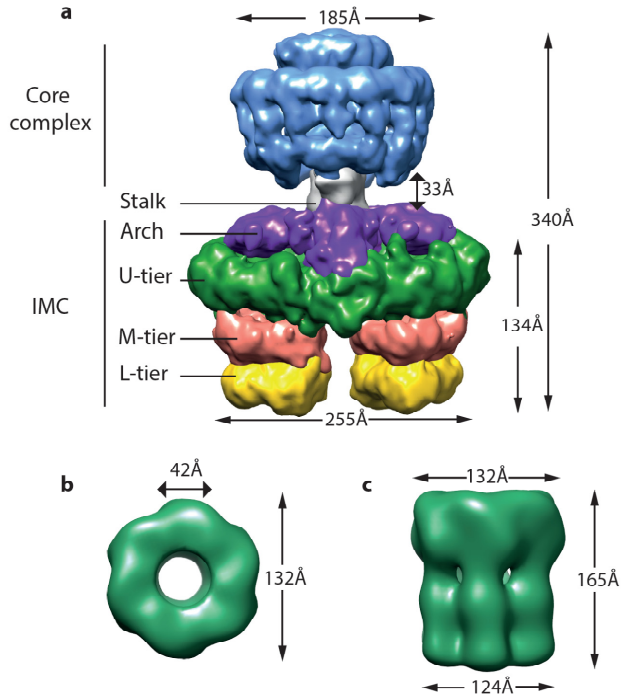

Figure 6. The NS-EM structure of $T4SS_{3\text{-}10}$ complex (EMD-2567) from R388. (a) side view. (b) top view and (c) side view of the NS-EM reconstruction of VirB4 from R388 plasmid (EMD-5505).

6. Discussion and Future Directions

Significant progress has been made in understanding the architecture of the T4SS during the last decade [16,18]. The intensive structural studies have revealed a very distinct organisation of this secretion apparatus that spans both inner and outer-membranes and have localised different subunits within its structure. It has been shown that the OMCC is formed even in the absence of other T4SS components [26]. Moreover the T4S system formation is initiated by the assembly of the OMCC, which serves as a scaffold for the assembly of all the rest of the T4S components [48,49]. This complex might serve as a seed for the assembly of the other T4SS components. Detailed examination of the complete and truncated OMCCs indicates that VirB10 spans the entire cell envelope. This finding supports the hypothesis that ATP-driven conformational changes within N-terminus of VirB10 could serve as a gating mechanism in the T4SS channel [50,51]. Unfortunately, very little is

known about the connection between T4S channel components and ATPases and the composition of the IMC in general. The only available information has been derived from the recently obtained NS-EM reconstruction of the nearly complete T4SS from R388 [27] (Figure 7). However two ATPases, which are necessary for substrate recruitment and pilus biogenesis, VirD4 [52] and VirB11 [24], are not present within this structure. In order to understand the mechanism of substrate secretion, it is important to localize the missing ATPases with respect to the already assembled $T4SS_{3\text{-}10}$ complex as well as observe if their presence impact the overall structure of the T4S system.

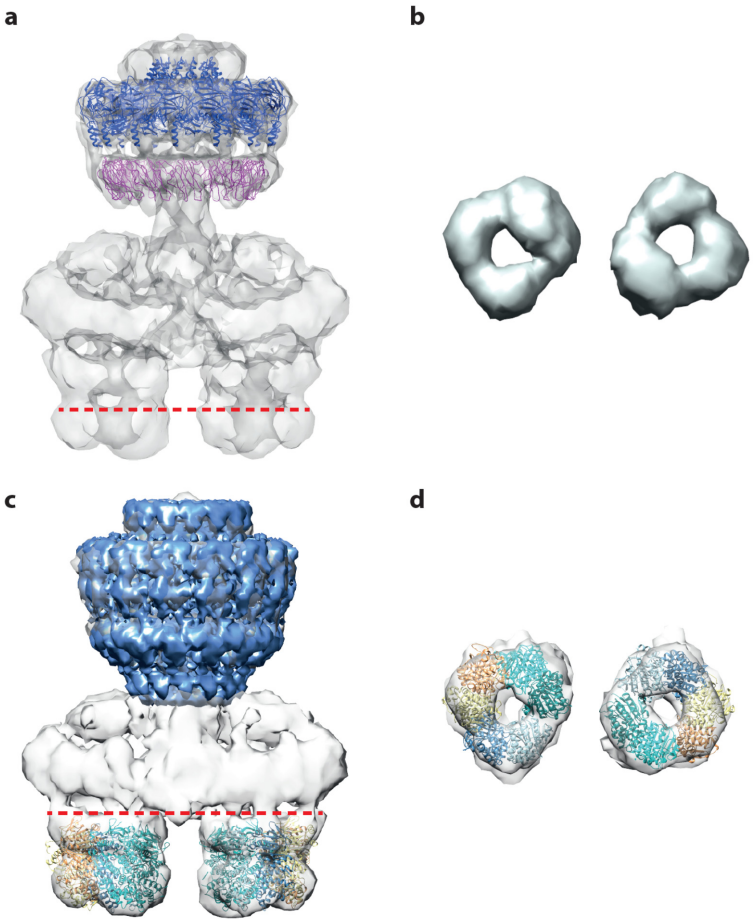

Figure 7. Comparison of the cryo and NS structures. (a) Side view of the NS-EM structure of $T4SS_{3\text{-}10}$ complex with fitted 14 TraF/$VirB10_{CT}$ subunits (PDB 3JQO) and the *in silico* model of the N-terminal domain of VirB9 from pKM101 (PDB 3ZBJ). (b) The view along the vertical axis from the inner membrane end reveals clear 3-fold symmetry of the barrels. (c) Side view of the NS-EM structure of $T4SS_{3\text{-}10}$ complex with fitted cryo-EM structure of the OMCC (Figure 4) and the VirB4 ATPase domain from *T. pseudethanolicus* (4AG5). (d) A cross section of the $T4SS_{3\text{-}10}$ complex in the area of the two barrels with fitted VirB4 ATPase domain.

The only information about the pathway of the substrate during the transfer so far comes from the *A. tumefaciens* VirB/D4 system [53]. However the molecular details of this process are still unknown and further investigations are required to understand how the T4S system interacts with and transport substrates through the bacterial envelope. A role and function of the pilus also requires more structural and biochemical studies. These tasks represent a great challenge that can only be met by implementing novel biochemical and genetic approaches resulting in trapping T4S systems at different stages of substrate transfer. The revealed organisation of the T4S systems is very unusual: contrary to other secretion systems such as T6SS, or T3SS the T4S systems do not have a rigid organisation based on the rotational symmetry of their major components or helical organisation [54,55,56].

7. Conclusions

Advances in the structural biology achieved by methods of electron microscopy helped to resolve structures of huge biological macromolecular complexes that are amenable to other structural methods. The combination of EM structures and biochemical approaches made possible localisation of important protein components within the structures and therefore provide validated suggestions on the T4S system possible mechanism of action. Hopefully the use of recently developed direct electron detection system, as well as improvement of the statistical analysis software in combination with novel biochemical methods will allow to elucidate the high resolution structure of the missing stalk region as well as the IMC with the ATPases [57,58]. These structural studies will be crucial to gain a complete understanding of the mechanism of T4SSs.

Acknowledgments

This work was funded by grant 082227 from the Wellcome Trust to GW and K012401 from MRC to EVO and GW. The authors would also like to thank the Wellcome Trust for the EM equipment.

Conflict of Interest

All authors declare no conflicts of interest in this paper.

References

1. Alvarez-Martinez CE, Christie PJ (2009) Biological diversity of prokaryotic type IV secretion systems. *Microbiol Mol Biol Rev* 73: 775–808.

2. Filloux A (2004) The underlying mechanisms of type II protein secretion. *Biochim Biophys Acta* 1694: 163–179.
3. Cornelis GR, Van Gijsegem F (2000) Assembly and function of type III secretory systems. *Annu Rev Microbiol* 54: 735–774.
4. Henderson IR, Navarro-Garcia F, Desvaux M, et al. (2004) Type V protein secretion pathway: the autotransporter story. *Microbiol Mol Biol Rev* 68: 692–744.
5. Cascales E (2008) The type VI secretion toolkit. *EMBO Rep* 9: 735–741.
6. Abdallah AM, Gey van Pittius NC, Champion PA, et al. (2007) Type VII secretion--mycobacteria show the way. *Nat Rev Microbiol* 5: 883–891.
7. Backert S, Meyer TF (2006) Type IV secretion systems and their effectors in bacterial pathogenesis. *Curr Opin Microbiol* 9: 207–217.
8. de Jong MF, Sun YH, den Hartigh AB, et al. (2008) Identification of VceA and VceC, two members of the VjbR regulon that are translocated into macrophages by the Brucella type IV secretion system. *Mol Microbiol* 70: 1378–1396.
9. Ninio S, Roy CR (2007) Effector proteins translocated by Legionella pneumophila: strength in numbers. *Trends Microbiol* 15: 372–380.
10. O'Callaghan D, Cazevieille C, Allardet-Servent A, et al. (1999) A homologue of the Agrobacterium tumefaciens VirB and Bordetella pertussis Ptl type IV secretion systems is essential for intracellular survival of Brucella suis. *Mol Microbiol* 33: 1210–1220.
11. Lederberg J, Tatum EL (1953) Sex in bacteria; genetic studies, 1945-1952. *Science* 118: 169–175.
12. Hofreuter D, Karnholz A, Haas R (2003) Topology and membrane interaction of Helicobacter pylori ComB proteins involved in natural transformation competence. *Int J Med Microbiol* 293: 153–165.
13. Ramsey ME, Woodhams KL, Dillard JP (2011) The Gonococcal Genetic Island and Type IV Secretion in the Pathogenic Neisseria. *Front Microbiol* 2: 61.
14. Lessl M, Lanka E (1994) Common mechanisms in bacterial conjugation and Ti-mediated T-DNA transfer to plant cells. *Cell* 77: 321–324.
15. Christie PJ, Cascales E (2005) Structural and dynamic properties of bacterial type IV secretion systems (review). *Mol Membr Biol* 22: 51–61.
16. Trokter M, Felisberto-Rodrigues C, Christie PJ, et al. (2014) Recent advances in the structural and molecular biology of type IV secretion systems. *Curr Opin Struct Biol* 27: 16–23.
17. Pansegrau W, Lanka E (1996) Enzymology of DNA transfer by conjugative mechanisms. *Prog Nucleic Acid Res Mol Biol* 54: 197–251.
18. Fronzes R, Christie PJ, Waksman G (2009) The structural biology of type IV secretion systems. *Nat Rev Microbiol* 7: 703–714.
19. Schmidt-Eisenlohr H, Domke N, Angerer C, et al. (1999) Vir proteins stabilize VirB5 and mediate its association with the T pilus of Agrobacterium tumefaciens. *J Bacteriol* 181: 7485–7492.

20. Schmidt-Eisenlohr H, Domke N, Baron C (1999) TraC of IncN plasmid pKM101 associates with membranes and extracellular high-molecular-weight structures in Escherichia coli. *J Bacteriol* 181: 5563–5571.
21. Christie PJ, Atmakuri K, Krishnamoorthy V, et al. (2005) Biogenesis, architecture, and function of bacterial type IV secretion systems. *Annu Rev Microbiol* 59: 451–485.
22. Eisenbrandt R, Kalkum M, Lai EM, et al. (1999) Conjugative pili of IncP plasmids, and the Ti plasmid T pilus are composed of cyclic subunits. *J Biol Chem* 274: 22548–22555.
23. Yuan Q, Carle A, Gao C, et al. (2005) Identification of the VirB4-VirB8-VirB5-VirB2 pilus assembly sequence of type IV secretion systems. *J Biol Chem* 280: 26349–26359.
24. Kerr JE, Christie PJ (2010) Evidence for VirB4-mediated dislocation of membrane-integrated VirB2 pilin during biogenesis of the Agrobacterium VirB/VirD4 type IV secretion system. *J Bacteriol* 192: 4923–4934.
25. Yeo HJ, Yuan Q, Beck MR, et al. (2003) Structural and functional characterization of the VirB5 protein from the type IV secretion system encoded by the conjugative plasmid pKM101. *Proc Natl Acad Sci U S A* 100: 15947–15952.
26. Fronzes R, Schafer E, Wang L, et al. (2009) Structure of a type IV secretion system core complex. *Science* 323: 266–268.
27. Low HH, Gubellini F, Rivera-Calzada A, et al. (2014) Structure of a type IV secretion system. *Nature* 508: 550–553.
28. Mossey P, Hudacek A, Das A (2010) Agrobacterium tumefaciens type IV secretion protein VirB3 is an inner membrane protein and requires VirB4, VirB7, and VirB8 for stabilization. *J Bacteriol* 192: 2830–2838.
29. Jakubowski SJ, Krishnamoorthy V, Cascales E, et al. (2004) Agrobacterium tumefaciens VirB6 domains direct the ordered export of a DNA substrate through a type IV secretion System. *J Mol Biol* 341: 961–977.
30. Judd PK, Mahli D, Das A (2005) Molecular characterization of the Agrobacterium tumefaciens DNA transfer protein VirB6. *Microbiology* 151: 3483–3492.
31. Thorstenson YR, Zambryski PC (1994) The essential virulence protein VirB8 localizes to the inner membrane of Agrobacterium tumefaciens. *J Bacteriol* 176: 1711–1717.
32. Sivanesan D, Baron C (2011) The dimer interface of Agrobacterium tumefaciens VirB8 is important for type IV secretion system function, stability, and association of VirB2 with the core complex. *J Bacteriol* 193: 2097–2106.
33. Terradot L, Bayliss R, Oomen C, et al. (2005) Structures of two core subunits of the bacterial type IV secretion system, VirB8 from Brucella suis and ComB10 from Helicobacter pylori. *Proc Natl Acad Sci U S A* 102: 4596–4601.
34. Bailey S, Ward D, Middleton R, et al. (2006) Agrobacterium tumefaciens VirB8 structure reveals potential protein-protein interaction sites. *Proc Natl Acad Sci U S A* 103: 2582–2587.

35. Ripoll-Rozada J, Zunzunegui S, de la Cruz F, et al. (2013) Functional interactions of VirB11 traffic ATPases with VirB4 and VirD4 molecular motors in type IV secretion systems. *J Bacteriol* 195: 4195–4201.
36. Wallden K, Williams R, Yan J, et al. (2012) Structure of the VirB4 ATPase, alone and bound to the core complex of a type IV secretion system. *Proc Natl Acad Sci U S A* 109: 11348–11353.
37. Pena A, Matilla I, Martin-Benito J, et al. (2012) The hexameric structure of a conjugative VirB4 protein ATPase provides new insights for a functional and phylogenetic relationship with DNA translocases. *J Biol Chem* 287: 39925–39932.
38. Durand E, Waksman G, Receveur-Brechot V (2011) Structural insights into the membrane-extracted dimeric form of the ATPase TraB from the Escherichia coli pKM101 conjugation system. *BMC Struct Biol* 11: 4.
39. Yeo HJ, Savvides SN, Herr AB, et al. (2000) Crystal structure of the hexameric traffic ATPase of the Helicobacter pylori type IV secretion system. *Mol Cell* 6: 1461–1472.
40. Savvides SN, Yeo HJ, Beck MR, et al. (2003) VirB11 ATPases are dynamic hexameric assemblies: new insights into bacterial type IV secretion. *EMBO J* 22: 1969–1980.
41. Llosa M, de la Cruz F (2005) Bacterial conjugation: a potential tool for genomic engineering. *Res Microbiol* 156: 1–6.
42. Schroder G, Krause S, Zechner EL, et al. (2002) TraG-like proteins of DNA transfer systems and of the Helicobacter pylori type IV secretion system: inner membrane gate for exported substrates? *J Bacteriol* 184: 2767–2779.
43. Gomis-Ruth FX, Moncalian G, Perez-Luque R, et al. (2001) The bacterial conjugation protein TrwB resembles ring helicases and F1-ATPase. *Nature* 409: 637–641.
44. Orlova EV, Saibil HR (2011) Structural analysis of macromolecular assemblies by electron microscopy. *Chem Rev* 111: 7710–7748.
45. De Carlo S, Harris JR (2011) Negative staining and cryo-negative staining of macromolecules and viruses for TEM. *Micron* 42: 117–131.
46. Dubochet J (2012) Cryo-EM--the first thirty years. *J Microsc* 245: 221–224.
47. Rivera-Calzada A, Fronzes R, Savva CG, et al. (2013) Structure of a bacterial type IV secretion core complex at subnanometre resolution. *EMBO J* 32: 1195–1204.
48. Jakubowski SJ, Kerr JE, Garza I, et al. (2009) Agrobacterium VirB10 domain requirements for type IV secretion and T pilus biogenesis. *Mol Microbiol* 71: 779–794.
49. Christie PJ (1997) Agrobacterium tumefaciens T-complex transport apparatus: a paradigm for a new family of multifunctional transporters in eubacteria. *J Bacteriol* 179: 3085–3094.
50. Cascales E, Christie PJ (2004) Agrobacterium VirB10, an ATP energy sensor required for type IV secretion. *Proc Natl Acad Sci U S A* 101: 17228–17233.
51. Banta LM, Kerr JE, Cascales E, et al. (2011) An Agrobacterium VirB10 mutation conferring a type IV secretion system gating defect. *J Bacteriol* 193: 2566–2574.

52. Zechner EL, Lang S, Schildbach JF (2012) Assembly and mechanisms of bacterial type IV secretion machines. *Philos Trans R Soc Lond B Biol Sci* 367: 1073–1087.
53. Cascales E, Christie PJ (2004) Definition of a bacterial type IV secretion pathway for a DNA substrate. *Science* 304: 1170–1173.
54. Schraidt O, Marlovits TC (2011) Three-dimensional model of Salmonella's needle complex at subnanometer resolution. *Science* 331: 1192–1195.
55. Kudryashev M, Wang RY, Brackmann M, et al. (2015) Structure of the Type VI Secretion System Contractile Sheath. *Cell* 160: 952–962.
56. Clemens DL, Ge P, Lee BY, et al. (2015) Atomic Structure of T6SS Reveals Interlaced Array Essential to Function. *Cell* 160: 940–951.
57. McMullan G, Faruqi AR, Henderson R, et al. (2009) Experimental observation of the improvement in MTF from backthinning a CMOS direct electron detector. *Ultramicroscopy* 109: 1144–1147.
58. Li X, Mooney P, Zheng S, et al. (2013) Electron counting and beam-induced motion correction enable near-atomic-resolution single-particle cryo-EM. *Nat Methods* 10: 584–590.